Whole-Building Airflow Network Characterization by a Many-Pressure-States (MPS) Technique

Peter R. Armstrong, P.E. **Donald L. Hadley**

Robert D. Stenner, Ph.D. **Michael C. Janus, P.E.**
Member ASHRAE

ABSTRACT

Applications of multizone airflow and contaminant dispersion models to specific buildings include air quality diagnosis, weatherization, smoke control, and pressure balancing for lab-hood safety. Research applications may involve energy and air quality impacts of infiltration and ventilation and development of associated standards. The benefits of these applications are not being fully realized because of uncertainties in model inputs. An economical test method that is as accurate but less intrusive and faster than incremental or component-by-component blower door testing is needed. Existing methods of measuring interzonal flows by tracers and flow-pressure network parameters by pressurization tests are reviewed in this paper. A method based on simultaneous measurement of all zone pressures within a given control volume and flow measurements on a few selected interzonal paths is presented. Flow rates at a subset of flow measuring locations are controlled during testing to take on two or more values. Constrained, nonlinear least squares analysis produces the power law parameters (flow coefficient and exponent) for each two-port aggregate flow path within the topology. Testing cost and effort are reduced by relying mainly on zone pressure measurements and a rich set of HVAC- or blower door-induced flow-pressure excitation states with relatively few flow measuring stations. Results of applying the method to a two-story test building are reported. Potential application to fault detection, acceptance testing, continuous commissioning, smoke dispersion, and other problems of building performance and operation are outlined.

INTRODUCTION

For over 50 years, researchers and weatherization contractors have performed blower door and tracer-gas tests on (mostly detached residential) buildings to estimate the energy and indoor air quality impacts of infiltration, ventilation, and envelope sealing (Dick 1950; Bahnfleth et al. 1957; Coblentz and Achenbach 1963). Similar equipment and procedures have been developed to estimate duct leakiness in the field. Recently, multiply controlled blower-door and multi-tracer-gas test equipment have been marketed to measure leakiness of individual zones and flows among zones within a building.

Multizone airflow network modeling became an important research area in the 1980s, developing in parallel with computational fluid dynamic (CFD) modeling of detailed air movements *within* zones. Applications of multizone modeling include indoor air quality (IAQ) and energy modeling, airborne hazard vulnerability assessment and mitigation, and moisture damage research and assessment. Real-time information about building airflows may be extremely useful to new advances in building operation, such as continuous commissioning, optimal control, fault detection and diagnosis, and other intelligent building functions.

However, two kinds of uncertainty persistently resist a modeler's efforts to accurately represent a specific multizone building. One of these—the specification of wind pressures—will not be addressed here. The other "impediment to the complex problem of predicting airflows in a multi-zone building ... has been the lack of reliable measurements of the flow resistances between the zones" (Modera and Herrlin 1990). In his list of the seven most pressing research activities, de Gids (1989) cites "pressure coefficients and air leakage data needs"

Peter Armstrong is a senior research scientist, **Donald Hadley** is a program manager, and **Robert Stenner** is a staff scientist at the Pacific Northwest National Laboratory, Richland, Wash. **Michael Janus** is a program manager for the Battelle Edgewood Office, Bel Air, Md.

second only to combining CFD and multizone models. Ten years later, leak parameters input to a model are still considered the main source of multizone modeling uncertainty (Sherman and Jump 2000); as simply stated in the *ASHRAE Handbook—Fundementals* (ASHRAE 1997): "determining the correct inputs to these models is difficult."

The foregoing assessments are based on variability among nominally identical dwelling units or envelope components reported in what most experts consider a woefully inadequate number of such field studies. "Little information on inter-zonal leakage has been reported because of the difficulty and expense of measurement" (ASHRAE 1997). Except for the handful of validation projects reported to date (see other papers of this symposium), reconciliation of measurements with a corresponding building airflow network model is rarely completed with any degree of scientific rigor, if at all.

It seems likely, therefore, that a practical means of obtaining accurate model input parameters for specific multizone buildings would motivate much wider and more effective use of zonal air movement and contaminant dispersion models in research as well as in the domains of building commissioning, operations, and retrofit.

REVIEW OF FIELD TEST PROCEDURES

Envelope leakiness is routinely measured in small buildings by blower-door testing using the single-fan pressurization technique. The procedure results in a power law relation (PLR) between leakage flow rate and indoor-outdoor pressure difference. Estimation of envelope PLR parameters from single-zone blower door data is a simple inverse problem.

Multiple fan pressurization techniques are sometimes used to measure interzonal air leakage. Modera and Herrlin (1990) developed a two-blower-door technique for measuring the interzonal leakage between two adjacent zones in a multizone building. Love (1990) has used three blower doors to measure separate envelope and party-wall leak parameters in row houses.

Single-fan measurements with incremental sealing can be used to identify flow parameters for multiple leakage paths. To be reasonably accurate, sealing must be executed in proper sequence (largest to smallest leaks). The method is tedious and often ends with 10% to 30% of the total ELA unaccounted for. Moreover, the destination ("to-zone") of leaks associated with a given pressurized zone ("from-zone") is often uncertain (Armstrong et al. 1996, 1997).

It is possible to determine overall leakiness of a building envelope by using the building's air-handling equipment to pressurize the whole building and a pulsed, constant-concentration, or constant-injection tracer gas technique to measure airflow through the fans or individual supply branches (Persily and Grot 1986; Persily and Axley 1990).

A number of tracer methods have been developed for measuring air infiltration rates into single zones and among multiple zones within a building. These include constant concentration single tracer gas systems, multi-tracer gas systems, and passive and active perfluorocarbon multi-tracer systems, capable of measuring average interzonal and multizonal airflows under changing flow and pressure conditions (Harrje et al. 1990). The tracer methods are generally intended to measure flow rates under naturally occurring stack-, wind-, and HVAC-developed pressure conditions. Airtightness parameters cannot be inferred because the variations in interzonal pressures are small. In fact, pressure measurement is not generally called for in the infiltration and ventilation test procedures that use tracer gas measurements. Inverse analysis is applied to the system of mass balance equations to estimate the interzonal flow rates during the multi-zone tracer test. But the system of mass balance equations involves only tracer injection rate and concentration response time-series data.

PROBLEMS WITH MODEL INPUT DATA

Multizone models such as CONTAM and COMIS[1] (Feustel and Dieris 1992) solve instantaneous flow rates and zone pressures at a given set of boundary conditions. Contaminant dispersion is then evaluated for a short time step. Transient simulations are executed by repeating the process for many successive time steps.

The hydrodynamic principles and algorithms of COMIS, CONTAM, and the others are well understood and universally accepted. The modeler's task is to correctly describe the building topology and all of its relevant parameters. Thoughtful user-interface design with graphical input of zone and path locations has made describing a building topology relatively easy. This leaves specification of the zone and airflow path parameters as the overwhelming, and seemingly unavoidable, balance of model setup work. Parameters describing all envelope leaks, zone volumes, temperatures, and elevations; interzonal leaks; air distribution topology, duct sizes and leak characteristics; and damper and fan characteristics must be provided.

For example, Musser and Yuill (1999) prepared a very detailed residential building model with 2000 zones and 7000 leakage paths to perform CONTAM simulations of residential infiltration rates. The vast majority of the leak paths are cracks in floor and wall constructions whose resistance can only be crudely estimated. For some research endeavors this uncertainty is not disabling: it may be sufficient to know that leakage area is distributed more or less uniformly or that aggregate leakage area is equal to some predetermined representative value. In other applications, however, the value of a simulation result depends critically on accurate representation of a specific building, i.e., on accurate specification of all interzonal and exterior envelope leak parameters. We know that variability in these parameters is large and that they are difficult to measure.

1. CONTAM and COMIS are widely used public-domain zonal airflow/IAQ modeling packages (Feustel and Dieris 1992).

In this paper, we develop a technique for identifying leak parameters in any building that can be modeled as discrete zones connected by airflow paths. The method relies on simultaneous pressure measurement in all zones within and at the boundaries of a specified control volume and requires relatively few airflow measurements. The zone pressures and (known and unknown) flow rates for a given network state describe *n* mass balance relations, where *n* is the number of zones. A large number of flow-pressure states can be obtained by varying each of several flow rates independently. Because of this distinguishing feature, we call this approach a *many pressure states* (MPS) technique. A constrained iterative search is used to find the power law relation (PLR) exponents that best satisfy (least sum of squared errors) the mass-balance equations for all states. The PLR coefficients are estimated at each iteration by linear least squares. The governing equations and the solution algorithm are developed, and results of numerical experiments are presented.

FORWARD PROBLEM FORMULATION

A leak path is characterized by an expression relating the pressure between its terminating points and the flow through it. Zonal airflow models often characterize leaks by a power law relation defined, for positive flows, by $Q = Cp^x$, where Q is the flow rate, C is a constant, p is the pressure difference between the connected zones, and x is an exponent between 0.5 for fully turbulent flow and 1 for purely laminar flow (Walton 1997; Walker et al. 1998). (All symbols used in this paper are defined in the nomenclature section that follows the conclusions.)

What is often considered a single leak is really a complex of flow elements connected in series or parallel or some combination. A window sash, for example, may have different crack widths at the top, bottom, and two sides. The flow-pressure characteristics could be separately measured and the results combined analytically, but it is usual to measure only the aggregate flow and fit a single PLR. Each parallel element can be further decomposed into a set of series elements; for example, there might be two sets of gaskets for the air to pass through. What we accept as being very adequately modeled by a simple two-parameter power law expression is often a complex network of series and parallel paths.

A *two-port path* is a network of any complexity that has only two external terminal nodes. The window sash, as described above, can be considered a two-port path because we can measure and model total leak rate as a function of inside (room node) to outside (ambient node) pressure difference. It is not hard to produce a large number of test cases in CONTAM to demonstrate that the flow-pressure character of most two-port paths of interest in building infiltration problems can be adequately modeled by a single PLR.

The airflow network is represented by a pressure-flow relation for each flow path and a mass balance equation for each node. The pressure drop across a two-port flow path is related to the associated zone pressures by:

$$p = (P_1 - P_2) + g(\rho_1 z_1 - \rho_1 z_2) \quad (1)$$

where

- p = pressure drop across flow path of interest
- P_1,P_2 = floor level pressures in from-zone and to-zone
- ρ = air density
- g = acceleration of gravity (9.81 m/s^2)
- z_1, z_2 = entry and exit elevations with respect to from-zone and to-zone floors.

Walton (1997) describes three variants of the empirical PLR flow-pressure relation:

Volumetric flow rate:

$$Q = Cp^n \quad (2a)$$

Mass flow rate:

$$F = Cp^n \quad (2b)$$

Root-density-corrected flow rate:

$$Q = (\rho_o/\rho)^{1/2} Cp^n \quad (2c)$$

where ρ_o = reference density. A mass balance for the *ith* zone is given by

$$\Sigma_{j \neq i}(F_{ij}) = e_i \quad (3)$$

where F_{ij} denotes an unknown flow, given by Equations (1) and (2b), or a specified flow (boundary condition), from the *jth* zone to the *ith* zone and $\Sigma_{j\neq}$ denotes summation over all from-zones. In Equation (3), *j* is the from-zone pointer and *i* is the to-zone pointer.

There are *n* unknown zone pressures and *n* linked mass balance equations (3) about the zones. The system of equations can be solved tediously by successive relaxation (Cross 1934) or very efficiently by the Newton-Raphson (N-R) procedure (Martin and Peters 1963; Walton 1984). In either case, the unknown zone pressures are adjusted at each iteration in a direction that will reduce the residual mass balance errors, e_i, $i=1:n$. Appendix A describes how N-R is efficiently applied to this special type of problem.

INVERSE PROBLEM FORMULATION

The inverse problem (with all flow elements modeled by PLRs) has *2m* unknowns, where *m* is the number of two-port paths and, typically, $m>>n$. The system consists—like the system of the forward problem—of a set of *n* linked mass balance equations, but the *n*-vector of pressures measured at one network flow state will not provide enough information to solve the *2m* unknowns. This system is underdetermined. By exciting the system in different ways, however, one may effectively produce replicates of the mass balance equations with different boundary conditions. Moreover, exciting the system in *many* different ways improves confidence intervals in a

manner analagous to the improvement obtained in any experiemnt by replication or by increasing the range and number of conditions tested. Least squares finds the best solution given data in which most of the measurement error is in the dependent[2] variable—in this case the flow measurements.

Mass Balance Equations. One way in which the inverse problem departs from the forward problem (wherein the pressures are unknown) is its use of pressure *differences* instead of zone pressures. The first step in the analysis is to convert zone pressures to flow element pressure differences after which the zone pressures are never again referenced. In the balance of this paper the phrase "flow path pressure" will be understood to mean "signed pressure difference across a given two-port flow element."

The mass balance for zone i is expressed very generally in terms of all flow element pressures p_j as follows:

$$\sum_{j=1}^{m} \delta_{i,j} C_j p_j^{x_j} = \sum_{j=1}^{m} \beta_{i,j} F_j \qquad (4)$$

where

m = number of two-port paths in the system

C_j, x_j = unknown parameters of the jth flow element

F_j = *measured* flow in the jth flow path

$\beta_{i,j}$ = (-1, 0, 1) = sign of the measured flow j into zone i

$\delta_{i,j}$ = (-1, 0, 1) = sign of the unmeasured flow j into zone i

The parameters β *and* δ establish the topology of the system. Nonzero values of $\delta_{i,j}$ are assigned only to those paths j connected to a given zone i. The usual sign convention is positive for a flow into the ith zone.

Every fan-induced flow into, out of, or between zones must be measured and assigned to the appropriate right-hand side (RHS) sum. It is theoretically possible to obtain a useful solution with just one of the equations having a nonzero value on the RHS, provided sufficient accuracy and richness of variation in pressure (wind, temperature, and fan-induced) boundary conditions. However, we expect that, in practice, the number of measured flows (corresponding to nonzero RHS terms) will have to be a substantial fraction of the number of zones. Note that for any passive *measured* flow j (e.g., at a return air grille flow station) the flow element parameters (C_j,x_j) are estimated by the usual blower-door flow-pressure regression independent of the flow-pressure network problem. The $\beta_{i,j}$'s and $\delta_{i,j}$'s corresponding to a measured passive flow are set to 0 and ±1, respectively, just as if it were a measured fan-induced flow.

Topology. Reliable specification of the topology matrices is difficult and tedious. To overcome this difficulty, we wrote a program that produces the topology matrices [$\beta_{i,j}$] and [$\_{i,j}$] by reading the CONTAM generated project description file corresponding to the user's building description. The topology matrices [$\beta_{i,k}$] and [$\_{i,k}$] may thus be conveniently generated by preparing a CONTAM model for any building of interest. Multiple paths between a given pair of CONTAM zones must be aggregated into a single two-port path. Only zones with measured pressures can be admitted to the model. The CONTAM model (.ndf file) will list m paths. Each *measured* flow is represented by a constant mass flow rate (fan) element or by a supply or return register associated with a simple[3] air handler.

A mix of fan and supply register flow elements may be used to excite the system. The air source/sink for a fan may be zone 0 (outside ambient) or the fan may induce airflow between any pair of (usually adjacent) zones. A flow element representing the aggregate of *unmeasured* passive flows between adjacent zones may also be included in the model as a separate flow-pressure relation with unknown parameters. This situation is reflected in the topology vectors when [δ] contains a nonzero element corresponding to a nonzero element of β, i.e., $|\delta_{i,j}| = |\beta_{i,j}| = 1$ for a particular i and j.

A second program was written to produce "data" for initial testing of the inverse analysis. The latter program generates a large number of unique flow excitation states and calls CONTAMX[4] to solve the flow-pressure network at each state.

If the exponent x of each power law relation is specified, the overdetermined system of equations (Equation 4) is linear and the PLR coefficients C can be readily solved by linear least squares. Assuming leak locations and types are known with some confidence, one can, for example, assign an exponent of 0.5 to cracks and other openings wider than a few mm (0.1 in.), 0.65 to small cracks, and 0.8 to porous flow elements. The power law coefficients determined by least squares will be quite sensitive to the exponent estimates but the ELAs much less so. One test of this approach —described later in the paper (Test 3 shown in Figure 4)—resulted in root-mean-square (rms) deviation of less than 1% from true flow and maximum deviation of less than 2% from true flow.

In cases where it is important that the *exponents*, as well as the power law *coefficients*, be determined from field data, the least squares model fitting criterion is still appropriate but the linear least squares *algorithm* is not. Various optimization methods are available to solve nonlinear least squares problems (Gill et al. 1981). Most of the results reported in this

2. Random error in the *independent* variables will result in biased parameter estimates as will bias in any of the measurements: thus the universally understood need to avoid measurement bias at any reasonable cost.

3. CONTAM's "simple air handler" model provides a specified constant flow rate at each register.

4. CONTAMX (public domain) is the solver portion of CONTAM and is command-line callable.

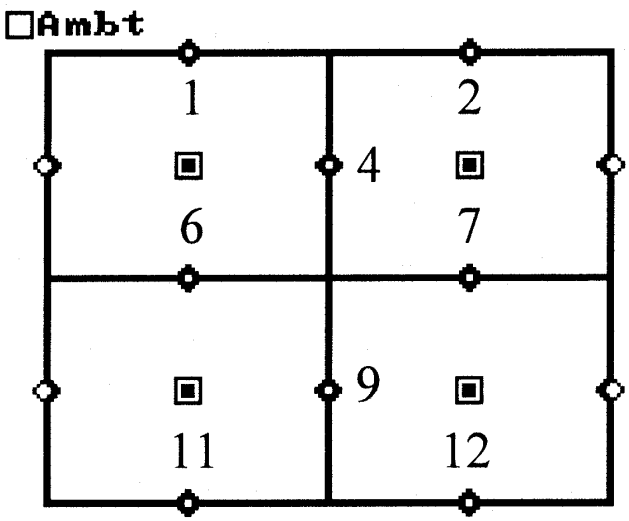

Figure 1 *Floor plan of the simulated four-zone, one-story house. Diamonds represent leaks, half-diamonds represent fans, and boxes represent zones.*

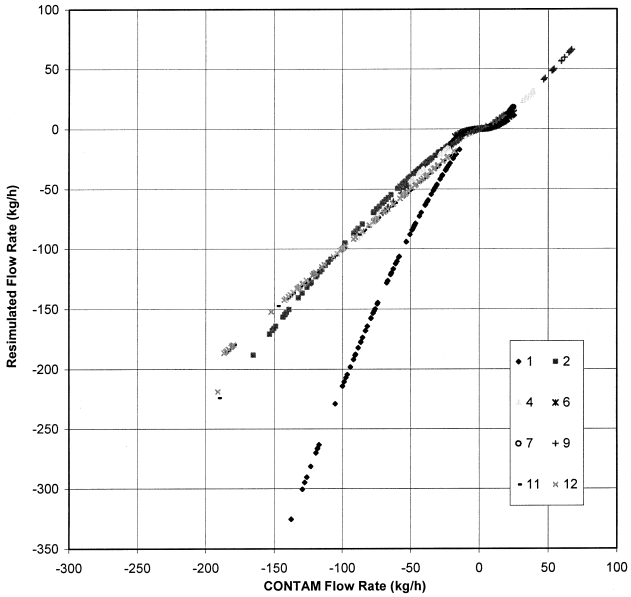

Figure 2 *Comparison of predicted flow rates vs. "measured" flow rates for Test 1. The CONTAM flow rates serve as the "measured data" and the resimulated flow rates are obtained by evaluating the least-squares PLRs for each pressure condition in the data set.*

paper have been obtained by the simple constrained steepest descent algorithm presented in Appendix B.

TEST RESULTS USING SIMULATED PRESSURES

The problem formulation (Equation 4) and parameter estimation algorithms were tested initially using simulated field data produced by CONTAM for a four-zone, one-story house. The floor plan is shown in Figure 1 and the flow rates used to excite the system are presented in Table 1. Complete enumeration of three flow rates at each of the four induced-flow locations results in 81 (3^4) flow-pressure states. Because there are four mass balance equations, the least squares data set consists of 324 (81 · 4) "data points."

The regression estimates of the flow coefficients for three scenarios applied to the same eight-flow-path topology are shown in Table 3.[5] In Test 1, we assumed that all the "unknown" power law exponents are equal to one. The flows predicted by the model for each state are plotted in Figure 2. For two of the three "large" flows and two of the three "intermediate" flows, the flows are predicted quite well. The two "small" flows exhibit large nonlinear deviations.

In Test 2, we assume that $x = 0.75$ for all power law exponents. In Test 3 we apply some plausible estimates of the expo-

5. The coefficients C reported in Tables 3-5 and Table 7 in SI units have a physical interpretation and their accurate measurement is, of course, the main objective of the proposed method. However, their absolute values are not useful in assessing performance of the method—rather it is the *relative* deviations of the coefficients from the values reported in the "actual" column. We therefore beg the reader's indulgence, in the name of time, space, ink, and paper, for omitting the corresponding I-P values.

TABLE 1
CONTAM Flow-Pressure Parameters for Tests 1 through 11 (see Table 2 for Constant Mass Fan Parameters)

Flow Path #	Element Type	*C* kg/h per (Pa)^x	*C* scfm per (in.wc)^x	*x* dimensionless
1	2 windows	13.47	449.7	0.76497
2	window	6.735	224.9	0.76497
3	fan1			
4	tight door	6.735	224.9	0.76497
5	fan2			
6	loose door	3.069	102.5	0.50000
7	loose door	3.069	102.5	0.50000
8	fan3			
9	tight door	6.735	224.9	0.76497
10	fan4			
11	window	6.735	224.9	0.76497
12	window	6.735	224.9	0.76497

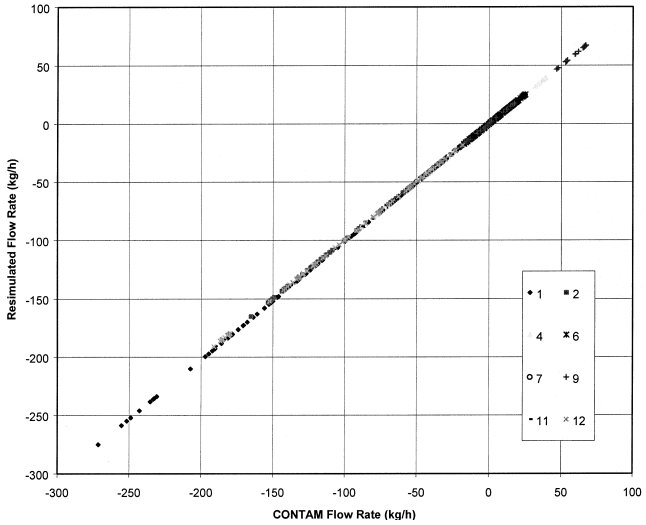

Figure 3 *Comparison of predicted flow rates vs. "measured" flow rates for Test 3. The CONTAM flow rates serve as the "measured data" and the resimulated flow rates are obtained by evaluating the least-squares PLRs for each pressure condition in the data set.*

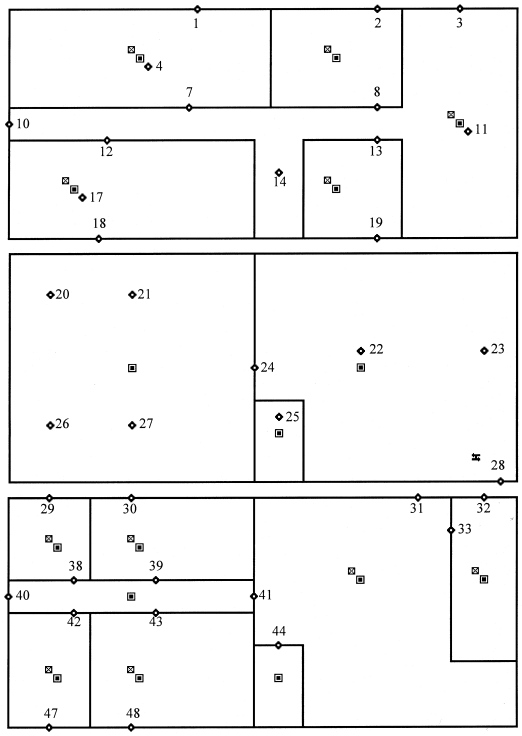

Figure 4 *Model plan views of the simulated 16-zone, two-story office. Bottom panel shows 1st floor, center panel shows 1st floor ceiling plenum, top panel shows 2nd floor. Each supply air register is represented by a boxed x. All room return grilles are sealed and fan intake is arranged for 100% outside air with the return duct closed off.*

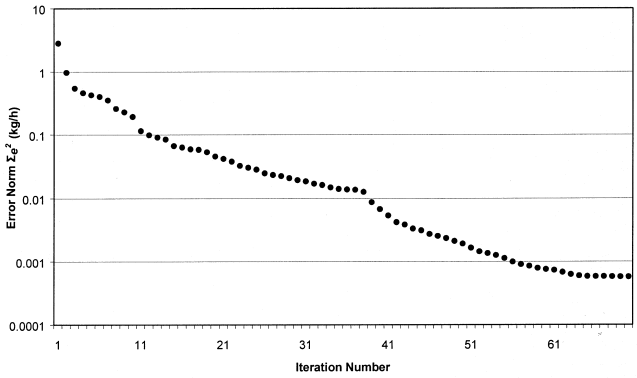

Figure 5 *Convergence of the mean-square norm of mass-balance residuals for Test 12.*

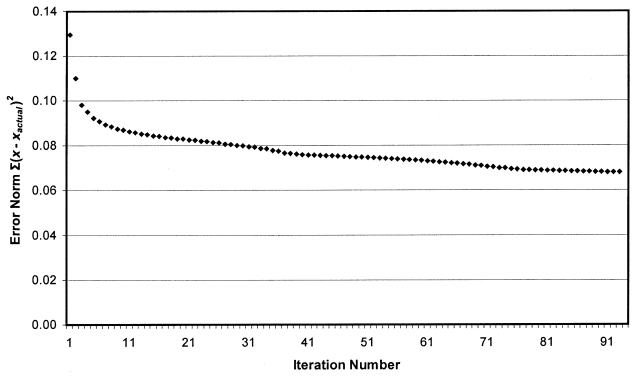

Figure 6 *Convergence of the PLR exponents for Test 12.*

TABLE 2
Excitation Grid Mass Flow Rates for Tests 1 through 7

Flow Path #	Element	Excitation Flow Rates (kg/h)			Excitation Flow Rates (scfm)		
3	fan1	204.6	61.4	20.5	100	30	10
5	fan2	204.6	61.4	20.5	100	30	10
8	fan3	204.6	61.4	20.5	100	30	10
10	fan4	204.6	61.4	20.5	100	30	10

nents (see Table 3). Not surprisingly, given that "perfect" data are provided as input, least-squares regression predicts the eight flows almost perfectly, as shown in Figure 3. The rms deviation is less than 1% of true flow and maximum deviation is less than 2% of true flow for all 81 states.

The next four tests demonstrate the hybrid search algorithm that finds all the PLR parameters simultaneously. Test 4 assumes perfect "data," i.e., no measurement noise. In Tests 5 through 7, a series of models are identified from data sets with increasing levels of random noise added. Results are presented in Table 4.

In Tests 8 through 11, the number of excitation states is reduced from the 81 states used in previous tests to 36 and 16. The results are presented in Table 5.

A small office building with 16 zones and 37 aggregate two-port paths was modeled to give the inverse analysis procedure a more realistic test. The floor plans are shown in Figure 4. Excitation grid flow rates used in Tests 12 and 13 are presented in Table 6. Test 12 is for perfect flow and pressure data, and Test 13 is for flow measurements having a coefficient of variation of 10% and pressure measurements having a coefficient of variation of 5%. The simulated errors are

TABLE 3

Coefficients, C (kg/h/Pa^x) Estimated with Prespecified Exponents.

			Test 1			Test 2			Test 3		
Standard error (kg/h):			**12.04**			**2.08**			**0.202**		
Flow Path		C_{actual}									
#	**Element**	**kg/h/Pa^x**	***x***	***C***	***t***	***x***	***C***	***t***	***x***	***C***	***t***
1	2 windows	13.47	1.00	5.93	93	0.75	14.17	551	0.76	13.44	5685
2	window	6.735	1.00	2.87	55	0.75	7.11	323	0.76	6.72	3318
4	tight door	6.735	1.00	3.12	34	0.75	7.04	213	0.76	6.72	2189
6	loose door	3.070	1.00	0.20	4	0.75	1.35	68	0.50	3.06	681
7	loose door	3.070	1.00	0.28	6	0.75	1.34	76	0.50	3.07	765
9	tight door	6.735	1.00	3.26	40	0.75	7.02	244	0.76	6.72	2510
11	window	6.735	1.00	2.83	65	0.75	7.07	366	0.76	6.72	3863
12	window	6.735	1.00	2.76	72	0.75	7.08	411	0.76	6.72	4283

TABLE 4

Coefficients *C* (kg/h/Pa^x) and Exponents *x* Estimated by Nonlinear Least Squares with 81 Excitation States; Results are Shown for Clean and Noisy Data

				Test 4		Test 5		Test 6		Test 7	
Zone Flow Noise (σ/μ%)				**0**		**2**		**5**		**10**	
Pressure Noise (σ/μ%)				**0**		**0**		**2**		**5**	
Standard error of fit (kg/h)				**0.003**		**2.78**		**7.29**		**11.37**	
Flow Path											
#	**Element**	x_{actual}	C_{actual}	***x***	***C***	***x***	***C***	***x***	***C***	***x***	***C***
1	2 windows	0.765	13.47	0.765	13.25	0.766	13.37	0.771	13.03	0.790	7.17
2	window	0.765	6.735	0.764	6.738	0.771	6.61	0.744	7.17	0.713	4.46
4	tight door	0.765	6.735	0.766	6.701	0.760	6.79	0.812	5.86	0.871	2.16
6	loose door	0.500	3.070	0.499	3.077	0.516	2.86	0.497	2.89	0.602	1.16
7	loose door	0.500	3.070	0.505	3.019	0.544	2.70	0.520	2.91	0.769	5.25
9	tight door	0.765	6.735	0.769	6.635	0.755	6.84	0.759	6.73	0.799	6.11
11	window	0.765	6.735	0.765	6.720	0.767	6.64	0.765	6.74	0.763	5.87
12	window	0.765	6.735	0.764	6.734	0.772	6.54	0.774	6.49	0.775	7.18

TABLE 5
Coefficients *C* (kg/h/Pa^x) and Exponents Estimated with Fewer Excitation States

				Test 8		Test 9		Test 10		Test 11	
Number of Excitation States				**36**		**36**		**16**		**16**	
Zone Flow Noise (σ/μ%)				**0**		**10**		**0**		**10**	
Pressure Noise (σ/μ%)				**0**		**5**		**0**		**5**	
Standard error of fit (kg/h)				**0.31**		**16.15**		**0.47**		**13.97**	
Flow Path											
#	**Element**	x_{actual}	C_{actual}	x	C	x	C	x	C	x	C
1	2 windows	0.765	13.47	0.764	13.52	0.783	12.53	0.763	13.56	0.986	5.53
2	window	0.765	6.735	0.764	6.77	0.597	11.91	0.762	6.82	0.733	7.17
4	tight door	0.765	6.735	0.765	6.74	0.849	4.99	0.763	6.77	0.872	3.14
6	loose door	0.500	3.070	0.532	2.77	0.678	1.72	0.537	2.71	0.271	5.73
7	loose door	0.500	3.070	0.533	2.76	0.624	2.93	0.543	2.68	0.756	1.07
9	tight door	0.765	6.735	0.756	6.91	0.659	9.06	0.720	7.63	0.717	8.68
11	window	0.765	6.735	0.763	6.78	0.724	7.95	0.764	6.78	0.704	8.93
12	window	0.765	6.735	0.762	6.81	0.738	7.29	0.761	6.84	0.710	8.66

TABLE 6
Excitation Grid Flow Rates for 16-Zone, 37-Path Tests

Flow Path					
#	**Element***	**Excitation Levels (kg/h)**		**Excitation Levels (scfm)**	
4	SA1	204.6	61.4	100	30
5	SA2	144		70.4	
9	SA3	204.6	61.4	100	30
15	SA4	180	54	88	26.4
16	SA5	126		61.6	
34	SA6	108	324	52.8	158.4
35	SA7	90	288	44	140.8
36	SA8	216	72	105.6	35.2
37	SA9	204.6	61.4	100	30
45	SA10	144	46.8	70.4	22.9
46	SA11	118.8		58	

* Supply air register numbers do not correspond to zone numbers. The zones whose supply registers are blocked throughout the testing are not listed.

TABLE 7
Coefficients (kg/h/Pa^x) and Exponents Estimated for 16-Zone, 37-Path Tests

				Test 12		Test 13	
Number of States:				**256**		**256**	
Zone Flow Noise σ/μ %:				**0**		**10**	
Pressure Noise σ/μ %:				**0**		**5**	
Standard Error (kg/h):				**0.16**		**9.3**	
Flow Path		**actual**					
#	**Element***	***x***	***C***	***x***	***C***	***x***	***C***
1	window	0.765	13.47	0.763	13.58	0.748	12.73
2	window	0.765	13.47	0.719	15.78	0.691	15.15
3	window	0.765	26.94	0.663	5.512	0.535	5.67
6	FlrDeck	0.950	29.89	0.950	35.56	0.947	26.40
7	IntDoor	0.500	6.139	0.511	5.847	0.602	3.65
8	IntDoor	0.500	3.069	0.710	1.325	0.689	1.23
10	ExtDoor	0.765	6.557	0.809	25.39	0.838	20.98
11	FlrDeck	0.950	29.89	0.947	47.3	0.941	26.86
12	IntDoor	0.500	3.069	0.532	2.795	0.617	1.90
13	IntDoor	0.500	3.069	0.701	1.495	0.689	1.33
14	IntDoor	0.500	3.069	0.706	3.957	0.691	2.05
17	FlrDeck	0.950	29.89	0.949	29.91	0.948	26.41
18	window	0.765	20.20	0.763	20.32	0.759	18.21
19	window	0.765	13.47	0.714	15.81	0.690	14.96
20	SATceiling	0.650	71.97	0.653	71.39	0.649	63.61
21	SATceiling	0.650	143.9	0.650	143.6	0.650	126.93
22	SATceiling	0.650	463.5	0.650	460.8	0.649	414.13
23	SATceiling	0.650	119.5	0.645	118.5	0.646	106.43
24	1.5"x24'gap	0.500	29.47	0.502	29.03	0.504	25.84
25	IntDoor	0.500	3.069	0.712	3.999	0.689	2.10
26	SATceiling	0.650	98.51	0.646	97.91	0.652	86.94
27	SATceiling	0.650	197.1	0.649	197.6	0.649	172.05
28	ExtDoor	0.765	6.557	0.782	6.175	0.780	5.51
29	window	0.765	6.735	0.738	7.63	0.746	6.84
30	window	0.765	6.735	0.740	7.587	0.746	6.90
31	window	0.765	33.68	0.764	33.65	0.771	29.33
32	window	0.765	13.47	0.762	13.55	0.758	12.10
33	IntDoor	0.500	3.069	0.692	3.614	0.684	1.40
38	IntDoor	0.500	3.069	0.653	1.534	0.674	0.66
39	IntDoor	0.500	3.069	0.668	1.399	0.678	0.53
40	ExtDoor	0.765	6.557	0.941	3.385	0.780	2.90

TABLE 7 (Continued)
Coefficients (kg/h/Pa^x) and Exponents Estimated for 16-Zone, 37-Path Tests

41	IntDoor	0.500	3.069	0.619	2.808	0.668	1.76
42	IntDoor	0.500	3.069	0.627	1.928	0.663	1.25
43	IntDoor	0.500	3.069	0.623	2.005	0.663	1.29
44	IntDoor	0.500	3.069	0.711	4.02	0.689	2.15
47	window	0.765	6.735	0.739	7.449	0.742	6.64
48	window	0.765	13.47	0.758	13.88	0.748	12.74

* The user-assigned CONTAM flow element names refer, in this case, to the six hypothetical leak types – window, interior door, exterior door, floor deck, suspended acoustic tile ceiling, and a 1.5 in. gap – used in the 16-zone test case. Each instance of a given element is modified by a multiplier. For example, C takes on values of $1C_w$, $2C_w$, $3C_w$, etc., where C_w= 6.735 is the PLR coefficient for a single window and the multiples correspond to two-port paths consisting of 1, 2, and 3 window units that present 1, 2, or 3 parallel paths between a given pair of adjacent zones. The parameters estimated from noisy data naturally do not exhibit this perfect integer multiplicity.

random deviates of the normal distribution in both cases. Estimated coefficients (kg/h/Pa^x) and exponents for the two 16-zone, 37-path tests are presented in Table 7.

Progress towards convergence may be measured in terms of the mean of squared mass balance errors. This is shown for Test 12 in Figure 5. Reliable convergence tests usually involve the rate of change of the parameters, x, from iteration to iteration as well. Since we know the true values of the parameters that generated the "measured" data, the progress of parameters toward their true value can be shown. Convergence of the PLR coefficient estimates is not particularly meaningful because the coefficients are highly sensitive to exponent deviations and are obtained, in any event, by the direct solution method of ordinary least squares. The magnitudes of exponent deviations, on the other hand, do provide a useful picture of the solution process. Progress of the mean of the squared exponent errors is plotted for Test 12 in Figure 6.

The foregoing results indicate that the power law parameters can be reliably estimated in the presence of random flow and pressure measurement noise, that it is not necessary to establish active flow control in every zone, and that parameter estimates can be obtained from field data involving a manageable number of excitation states.

APPLICATION

Demonstration of a multi-pressure-states technique in a real building is the next important development step. Some equipment and procedural questions that we will face in the first implementation are considered below.

Flows into selected zones and between selected zone pairs can be induced by traditional blower door equipment or by adapting an existing air distribution system to the purpose. When using blower door equipment, the typical implementation will require that all zone supply, return, and exhaust registers be sealed (and all fans made inoperative) during tests. If the distribution system is used, all active supply and return zone flow rates must be measured. Some of the supply registers may be sealed and the return system may be totally disabled to reduce the number of flow control/measurement stations involved. If duct leakage is significant, it must be characterized (Francisco and Palmiter 2001) and duct pressures sampled simultaneously with zone pressures so that leakage flow rates can be evaluated for each flow excitation state. This characterization is needed to model the flow-pressure network during fan operation in any event.

Accuracy of the MPS method will be sensitive to the choice of excitation states. An ideal set of excitation states would result in a logarithmically uniform distribution of positive and negative pressure differences across each two-port path. Because the MPS user's ultimate purpose is to construct a building-specific model, preparation of such a model, using best *a priori* estimates of the PLR parameters, does not constitute additional work. The preliminary model can be used to select the minimum number of excitation flow/measurement stations that are likely to meet the model parameter accuracy requirements and to automatically generate the flow rates associated with the excitation states that result in good distribution of all path pressure drops. The trade-off between number of flow stations (equipment cost) and number of excitation states (test duration) may also be considered by running test cases through the preliminary model.

Accurate simultaneous measurement of a large number of pressures, while less challenging than measuring a similar number of airflows, will represent a significant instrumentation investment of hundreds of dollars per zone. Temperature-density corrections must be applied to sampling tubes with vertical runs. Continuing progress in cost-performance value of off-the-shelf sensitive, stable pressure transducers is helping the situation. The prospect of wireless absolute pressure sensors of sufficient accuracy is particularly intriguing for future applications. Temperature-density correction of the power-law coefficients will necessitate measurement of air temperature in all zones if there are significant, e.g., 6°C (10°F), variations.

We believe that experience will demonstrate the importance of interactive flow network modeling to rapid acquisition of a network's main flow path characteristics and to the resolution of problem zones and flow paths. These problem

flow elements typically need testing over wide flow or pressure ranges or require greater concentration of local flow and pressure measurement points in a particular subset of zones, duct networks, and chase, plenum, or framing cavities. The expense of making such measurements exhaustively throughout an entire building would rarely be justified. But with interactive analysis of building airflows and pressures, the few areas where such detailed measurements are really needed can be quickly identified in the field. Additional detailed measurements become very cost-effective when it takes only a few such measurements to reward the analyst with a significant reduction in uncertainty.

In Tests 1 through 12 we have treated the residual of each mass balance equation with equal weight. There is some indication that the *ratio* of residual to total zone flow may give "better" results. Adapting the embedded least-squares routine to compute weighted least-squares power law coefficients presents no great difficulty. The benefits and details of this approach, however, will have to be assessed with extensive field data. The sensitivity of results to errors in the independent variables (pressure differences, which must be relatively error free to obtain the good statistical properties customarily attributed to ordinary least squares) should also be assessed and possibly addressed by a modification of the least squares analysis known as *total least squares*.

Analysis of large, complex networks will tax computing resources in terms of both memory and execution time. Such networks can be decomposed into arbitrarily small subnetworks with known boundary conditions. However, problems can be expected when the sample sizes are effectively reduced in pursuing this simplifying measure. Least-squares parameter estimation can be expected to return the best results when applied to control volumes with many zones, measured flow rates, and excitation states.

CONCLUSION

Zonal modeling has been used widely to estimate energy and IAQ impacts in infiltration and ventilation, analyze smoke management and contaminant dispersion, and conduct research into new construction techniques, test methods, and building standards. Building-specific modeling is important to such varied applications as balancing lab hood and smoke control systems, building acceptance and evaluation, diagnosis of IAQ and moisture problems. Leak parameters input to a multi-zone model are frequently cited as the greatest source of uncertainty in predicting flow and air change rates.

Interzonal leak characterization by traditional blower-door methods is difficult and intrusive. Many leak sites are inaccessible, and it is difficult to isolate the myriad flow paths between zones. The number and aggregate magnitude of unknown and unintended flow paths is invariably and surprisingly large. Acquisition of complete leakiness data and reconciliation of measurements with a corresponding building airflow network model is, therefore, rarely accomplished with analytical rigor, if attempted at all.

To address these problems, an alternative method, based on simultaneous measurement of pressures in all zones and flow measurements on selected paths, has been developed. A constrained, nonlinear least squares analysis is used to obtain power law parameters (flow coefficient and exponent) for each two-port aggregate flow path defined in the topology. The governing equations and an efficient parameter estimation algorithm have been presented. Numerical "experiments" with the algorithm give very encouraging results. There is considerable flexibility inherent in a many-pressure-states technique. Practical implementations will tend to maximize the ratio of interzonal leak parameters acquired to flow stations deployed by relying mainly on zone pressure measurements and a rich set of flow-pressure excitation states. Cost and effort are reduced because pressure measurement is less costly and intrusive than flow measurement.

ACKNOWLEDGMENTS

The authors are indebted to David Chassin, Graham Parker, and Sue Arey at the Pacific Northwest National Laboratory and Bob Rudolph at Battelle's Edgewood Office who generously shared their time and expertise during the development of this work and review of the final manuscript. DOE's Laboratory-Directed Research and Development program supported the work reported here.

NOMENCLATURE

C_i = coefficient of power law flow-pressure relation for *ith* two-port flow path

d	=	distance (from previous search point) along current line of steepest descent
F_i	=	measured flow associated with the *ith* zone,
$J(\boldsymbol{x}) = \Sigma e^2$	=	mass balance error norm evaluated at $\boldsymbol{x} = [x_i]$
p_i	=	signed pressure difference across *ith* flow path
P_i	=	absolute pressure at the floor of zone *i*
R	=	maximum distance to search on the current line of steepest descent
r_i	=	positive distance beyond which the *ith* constraint is violated
u_i i^{th}	=	element of the steepest descent unit direction vector, $\boldsymbol{u}$
x_i	=	exponent of power law flow-pressure relation for *ith* two-port flow path
β_i 0 (-1, 0, 1)	=	cell (*ith* element) of vector that maps measured flows to zones
δ_i 0 (-1, 0, 1)	=	cell of vector that maps unmeasured (2-port leak) paths to zones.

REFERENCES

Armstrong, P.R., J.A. Dirks, Y. Matrosov, J. Olkinaru, and D. Saum. 1996. Infiltration and ventilation in Russian multi-family buildings. *ACEEE Summer Study on Energy Efficiency in Buildings.*

Armstrong, P.R., B.Y. Nekrasov, and I. Sultanguzin. 1997. Infiltration leak characterization by blower door tests. Report to the Foundation for Enterprise Restructuring and Financial Institutions Development, Moscow.

ASHRAE. 1997. *1997 ASHRAE Handbook—Fundamentals*, Chapter 25, Ventilation and Infiltration. Atlanta: American Society of Heating, Refrigerating and Air-Conditioning Engineers, Inc.

Bahnfleth, D.R., T.D. Moseley and W.S. Harris. 1957. Measurement of infiltration in two residences. *ASHRAE Transactions* 63(2):439-452.

Coblentz, C.W., and P.R. Achenbach. 1963. Field measurement of air infiltration in ten electrically-heated houses. *ASHRAE Transactions* 69(1).

Cross, H. 1934. *Analysis of flow in networks of conduits and connectors*. Bulletin #286, U. Illinois, Engineering Experiment Station.

de Gids, W.F. 1989. A perspective on the AIVC. *Progress and trends in air infiltration and ventilation research*, 10th AIVC Conference, Dipoli.

Dick, J.B., Garston, Watford, and Herts. 1950. Measurement of ventilation using tracer gas technique. *J. HPAC*, May.

Feustel, H.E., and J. Dieris. 1992. A survey of airflow models for multi-zone structures. *Energy and Buildings* 18: 79-100.

Francisco, P.W., and L.S. Palmiter. 2001. The nulling test: A new measurement technique for estimating duct leakage in residential homes. *ASHRAE Transactions* 107(1).

Gill, P.E., W. Murray and M.H. White. 1981. *Practical optimization*. New York: Academic Press.

Golub, G. H., and C. F. Van Loan. 1996. *Matrix Computations*, 3rd edition. Baltimore: Johns Hopkins University Press.

Harrje, D.T., R.N. Dietz, M.H. Sherman, D.L. Bohac, T.W. D'Ottavio, and D.J. Dickerhoff. 1990. Tracer gas measurement systems compared in multifamily building. *Air change rate and airtightness in buildings, ASTM STP 1067*, M.H. Sherman, ed., pp. 5-20. Philadelphia: American Society for Testing and Materials.

Love, J.A. 1990. Airtightness survey of row houses in Calgary, Alberta. *Air change rate and airtightness in buildings*, ASTM STP 1067, M.H. Sherman, ed. Philadelphia: American Society for Testing and Materials.

Martin, D.W. and G. Peters. 1963. The application of Newton's method to network analysis by digital computer. *Journal of the Institute of Water Engineers* (U.K.), vol. 17.

Modera, M.P., and M.K. Herrlin. 1990. Investigation of a fan-pressurization technique for measuring interzonal air leakage. *ASTM STP 1067*, M.H. Sherman, ed., pp 183-192. Philadelphia: American Society for Testing and Materials.

Musser, A., and G.K.Yuill. 1999. Comparison of residential air infiltration rates predicted by single-zone and multizone models. *ASHRAE Transactions* 105(2).

Persily, A., and J. Axley. 1990. Measuring airflow rates with pulse tracer techniques. *Air change rate and airtightness in buildings, ASTM STP 1067*, M.H. Sherman, ed., pp 31-51. Philadelphia: American Society for Testing and Materials.

Persily, A.K., and R.A. Grot. 1986. Pressurization testing of federal buildings. *Measured air leakage of buildings, ASTM STP 904*, H.R. Trechsel and P.L. Lagus, eds., pp. 184-200. Philadelphia: American Society for Testing and Materials.

Sherman, M.H., and D. Jump. 2000. Energy conservation in buildings, Chapter 6.3, *Handbook of heating ventilation and air conditioning*, Jan Kreider, ed. CRC Press.

Walker, I.S., D.J. Wilson and M.H. Sherman. 1998. A comparison of the power law to quadratic formulations for air infiltration calculations. *Energy and Buildings* 27:293-299.

Walton, G.N. 1984. A computer algorithm for predicting infiltration and interzone airflows. *ASHRAE Transactions*, 90(1).

Walton, G.N. 1997. *CONTAM96—User Manual*, NISTIR 5385. Gaithersburg, Md.: National Institute of Standards and Technology.

APPENDIX A
STANDARD FLOW NETWORK SOLVER

The standard Newton-Raphson algorithm can be modified to exploit certain properties of the flow network problem. The residuals and partial derivatives are evaluated at each iteration in a three-step process: (1) the flows and partials with respect to pressure drop across each two-port path in the network are evaluated in one pass through the network path list[6] and may be stored in this same list; (2) the residual vector, $\boldsymbol{e}$, and its norm, $|\boldsymbol{e}|$, are evaluated in one pass through the nodes; (3) the lower triangular part of the array, $\boldsymbol{A}$, of partial derivatives (of each residual with respect to the pressure at each node) is evaluated by adding to the to Node partial accumulator and subtracting from the from Node partial accumulator each partial derivative term.

If the flow and derivative components were not precomputed in this way (steps 1, 2, and 3), each would end up being evaluated twice (for each of the two nodes associated with each path) during every N-R iteration. In step 2, the path terminal node pointers determine to which flow sum the path flow is added and from which sum it is subtracted.

6. The flow network can be completely specified by a list of zones, each described by floor elevation and air density, and a list of two-port paths, each described by C, x, from- and to-zone pointers, and from- and to-zone elevations. Each record of the path list may be used to hold, additionally during simulation, the path flow rate and its derivative with respect to pressure for the current vector pressure estimate $\boldsymbol{P}$.

Derivatives a_{ij} (*i*th zone flow with respect to the *j*th node pressure) are accumulated in a similar manner during the same pass through the path list. The derivatives with respect to pressure drops across paths can be evaluated analytically.

These simplifications to the general Newton-Raphson scheme are valid for physically realizable flow network problems where the derivative of the *i*th node flow residual with respect to the *j*th node pressure is equal to the derivative of the *j*th node flow residual with respect to the *i*th node pressure. The correction vector $\boldsymbol{w}$ is obtained by solving the linear system $\boldsymbol{Aw} = \boldsymbol{e}$. Any standard method for solving a set of linear equations may be used; however, a significant improvement in execution speed can be obtained by exploiting the symmetric and sparse-matrix properties of the gradient matrix (Martin and Peters1963; Walton 1997).

An improved estimate of the node pressures is obtained by evaluating $\boldsymbol{P} = \boldsymbol{P} + k\boldsymbol{w}$, where $k = 0.75$ (tests confirm that this value, recommended by Walton, generally results in the fewest iterations) is the relaxation coefficient. The new residuals and corresponding error norm are then computed by repeating steps 1 and 2. If the new norm exceeds the old norm, the relaxation factor is reduced by a scaling factor, *s-scale*, and the correction vector and corresponding error norm are reevaluated; this process is repeated until an error norm smaller than the previous error norm is obtained. Experience with many prototype buildings indicates that reductions of the correction vector typically occur in only a few percent of the iterations and that one reduction of the correction vector (with *s-scale* = 1.3) is sufficient to obtain an improved estimate of the node pressure vector.

APPENDIX B
CONSTRAINED STEEPEST DESCENT SEARCH

The search for the parameters that characterize a multizone flow network begins with an intitial estimate of *x*, the vector of all PLR exponents. Linear regression is applied to determine the mean-squared mass flow balance error as the exponents are perturbed one by one; the resulting gradient vector, $\boldsymbol{u}$, defines the steepest descent direction in power law exponent space. Linear regression is performed at points along this line to find the distance *d* to the minimum (mean squared error) point. However, *d* must be constrained by limiting $R = \|r\|$ such that the feasible region $0.5 \le r_i u_i \le 1.0$, within *x*-space is not violated. Finally, the new base point for the next high-level iteration is evaluated:

$$\boldsymbol{x} = \boldsymbol{x} + \boldsymbol{u}d$$

There are two levels of iteration: change of direction (based on the object function derivatives with respect to each exponent) occurs at the high level and a unidirectional search for a minimum occurs at the low level. The two iterative levels are concerned with the flow network *exponents* only. The power law *coefficients* are still determined by ordinary least squares for each evaluation of the error norm expressed as a function of exponents, i.e., for each partial derivative evaluation as well as for each trial in the unidirectional search for a minimum. The linear and nonlinear parts of the problem are said to be separable (Golub and Van Loan 1996). The nonlinear search algorithm, including now the constraints, has three main parts:

- evaluate steepest descent direction,
- determine maximum search distance that won't violate any exponent constraint,
- find, by interval bounding, a point on the search line that reduces the error norm.

The interval bounding task requires one or two evaluations of the object function for each interval reduction. The object function is the root-mean-square norm of the flow balance residuals, $J = \Sigma e^2$. If there is only one minimum point on the steepest descent line, the interval can be halved at each reduction. Initial experience indicates that the response surfaces are well-behaved, i.e., free of local minima.

The steepest descent direction is given by the unit vector $\boldsymbol{u} = [u_j]$ where:

$$u_j = -S\dot{J}_j ,$$

where

$$\dot{J}_j = \frac{\partial J}{\partial x_j} ,$$

and

$$S = \left[\sum_j^n \dot{J}_j^{\,2} \right]^{-1/2}$$

Each component u_j of the direction vector in which there is no slack (e.g., last trial value of the corresponding exponent was equal to 0.5 or 1.0 and sign of new u_j doesn't point the search away from the constraint surface) must be set to zero. The power law flow coefficients must be evaluated by ordinary least squares for each evaluation of each partial derivative, $\delta J/\delta_j$.

The range of the unidirectional search is determined by first evaluating distance to the nearest constraint for each exponent with nonzero u_j:

$$r_j = \max\left(\frac{x_{j\,\max} - x_j}{u_j}, \frac{x_{j\,\min} - x_j}{u_j} \right)$$

and selecting the minimum of these distances, ignoring no-slack ($r_j = 0$) components, to be the maximum feasible range:

$$R = min(r_1, r_2, \ldots, r_m)$$

The unidirectional search routine evaluates the object function for a series of diminishing distances, *d*, starting with $d = R$. The object function, $J(\boldsymbol{x} + \boldsymbol{u}d)$, is evaluated at each new distance and a test of recent (J,d) pairs determines on which

side of *d* the minimum lies. The routine successively reduces the minimum-bracketing interval (as long as the object function continues to drop) to a specified sub-interval, typically 0.001R.

Computational efficiency must be considered when the iterative search is applied to a network with a large number, *m*, of flow paths. Appropriate sparse matrix methods (Walton 1997) may be beneficially applied to the linear system involving the power law *coefficients* that must be solved at each iteration. Computational effort is on the order of m^3 for the linear least squares problem that must be solved several times at each point in the search for *x*. Note that the sparse matrix pattern is defined in the set of equations (4) by the left-hand-side topology matrix, [L].